Robotica (2007) volume 25, pp. 661–675. © 2007 Cambridge University Press
doi:10.1017/S0263574707003530 Printed in the United Kingdom

Algebraic methods in mechanism analysis and synthesis

Manfred L. Husty*, Martin Pfurner, Hans-Peter Schröcker and Katrin Brunnthaler

University Innsbruck, Institute of Basic Sciences in Engineering, Unit Geometry and CAD, Technikerstraße 13, A6020 Innsbruck, Austria.

(Received in Final Form: April 25, 2007. First published online: September 6, 2007)

SUMMARY

Algebraic methods in connection with classical multidimensional geometry have proven to be very efficient in the computation of direct and inverse kinematics of mechanisms as well as the explanation of strange, pathological behavior. In this paper, we give an overview of the results achieved within the last few years using the algebraic geometric method, geometric preprocessing, and numerical analysis. We provide the mathematical and geometrical background, like Study's parametrization of the Euclidean motion group, the ideals belonging to mechanism constraints, and methods to solve polynomial equations. The methods are explained with different examples from mechanism analysis and synthesis.

KEYWORDS: Kinematic mapping; Constraint manifold; Mechanism analysis; Mechanism synthesis; Bennett mechanism; 6R inverse kinematics; Overconstrained mechanism.

1. Introduction

There are many different mathematical methods in dealing with mechanism analysis and synthesis. Matrix and vector methods are most common to derive equations that describe the mechanisms (see, e.g., Angeles[1]). Generally, these methods have the disadvantage that one has to deal with sines and cosines, which are eliminated using half tangent substitutions. Within the last ten years, algebraic methods have become successful in solving problems in mechanism analysis and synthesis. One of the main reasons are the advances in solving systems of polynomial equations. Many algorithms have been developed, all of them heavily relying on the use of computer algebra systems (see, e.g., Dickenstein *et al.*[2]).

In mechanism science, it is important to find the simplest mathematical modeling of a mechanism, because the systems of equations describing the mechanisms are generally very complicated. Therefore, it seems advantageous to have additionally a geometrical setting for the interpretation of the equations. Kinematic image spaces provide such a setting. They have been introduced by W. Blaschke[3] and E. Study[4] and have been forgotten for long time. The main contribution of this overview paper is to show that geometric preprocessing and an understanding of the multidimensional geometry of kinematic image spaces is crucial to find simple sets of equations, which then can be solved efficiently using all the advances in computer algebra and the newly introduced methods in polynomial equation solving.

The paper is organized as follows: In the remaining part of the introduction, the mathematical background and the algebraic-geometric method to derive constraint equations for mechanism analysis and synthesis is provided. Section 2 gives then the application of the devised algorithms to mechanism analysis, especially the inverse kinematics of serial $6R$-chains and the determination of the motion of overconstrained mechanisms. Section 3 deals with the synthesis of Bennett mechanisms.

1.1. Study-model of SE(3)

Euclidean displacements $\mathcal{D} \in SE(3)$ can be described by (see Husty *et al.*[5] and McCarthy[6])

$$\mathcal{D}\colon \mathbf{x}' = \mathbf{A}\mathbf{x} + \mathbf{t} \tag{1}$$

where $\mathbf{x}'$ resp. $\mathbf{x}$ represent a point in the fixed resp. moving frame, $\mathbf{A}$ is a 3×3 proper orthogonal matrix and $\mathbf{t} = (t_1, t_2, t_3)^T$ is the vector connecting the origins of moving and fixed frame. Expanding the dual quaternion representation (see Section 3.3.2 of Husty *et al.*[5]) and using an operator approach, the matrix operator corresponding to the normalized dual quaternion $\mathbf{q} = (x_0, x_1, x_2, x_3)^T + \varepsilon(y_0, y_1, y_2, y_3)^T$ is given by

$$\mathbf{M} := \begin{bmatrix} 1 & 0 & 0 & 0 \\ t_1 & x_0^2 + x_1^2 - x_3^2 - x_2^2 & -2x_0x_3 + 2x_2x_1 & 2x_3x_1 + 2x_0x_2 \\ t_2 & 2x_2x_1 + 2x_0x_3 & x_0^2 + x_2^2 - x_1^2 - x_3^2 & -2x_0x_1 + 2x_3x_2 \\ t_3 & -2x_0x_2 + 2x_3x_1 & 2x_3x_2 + 2x_0x_1 & x_0^2 + x_3^2 - x_2^2 - x_1^2 \end{bmatrix} \tag{2}$$

where

$$\begin{aligned} t_1 &= 2x_0y_1 - 2y_0x_1 - 2y_2x_3 + 2y_3x_2, \\ t_2 &= 2x_0y_2 - 2y_0x_2 - 2y_3x_1 + 2y_1x_3, \\ t_3 &= 2x_0y_3 - 2y_0x_3 - 2y_1x_2 + 2y_2x_1. \end{aligned} \tag{3}$$

* Corresponding author. E-mail: manfred.husty@uibk.ac.at

The point $(x, y, z)^T$ is transformed to $(x', y', z')^T$ according to

$$(1, x', y', z')^T = \mathbf{M} \cdot (1, x, y, z)^T.$$

The entries (x_i, y_i) in the transformation matrix $\mathbf{M}$ have to fulfill the quadratic identity

$$x_0 y_0 + x_1 y_1 + x_2 y_2 + x_3 y_3 = 0 \tag{4}$$

and at least one x_i is different from 0. The lower right 3×3 submatrix of $\mathbf{M}$ is an element of the special orthogonal group, $SO(3)$ and the x_i are the Euler parameters. This representation of Euclidean displacements is sometimes called the Study representation, and the parameters x_i, y_i are called Study parameters. They allow the following multidimensional geometric interpretation: Eq. (4) defines a six-dimensional quadric hypersurface in a seven dimensional projective space P^7. This quadric S_6^2 is called the *Study-quadric* and serves as a point model for Euclidean displacements. The quadric S_6^2 is of hyperbolic type and has the following properties:

1. The maximal linear spaces on S_6^2 are three dimensional (generator spaces).
2. Each tangent space cuts S_6^2 in a five-dimensional cone.
3. The generator space $x_0 = x_1 = x_2 = x_3 = 0$ is one of the 3-spaces mentioned above but it does not represent regular displacements, because in this space, all Euler parameters are zero. Therefore, this space has to be cut out of S_6^2. A quadric with one generator space removed is called *sliced*.

A detailed treatment of more properties of S_6^2 can be found in Selig, Chapter 10.[7] The mapping

$$\begin{aligned} \kappa : \mathcal{D} &\to P \in P^7 \\ \mathbf{M}(x_i, y_i) &\to (x_0 : x_1 : x_2 : x_3 : y_0 : y_1 : y_2 : y_3)^T \\ &\neq (0 : 0 : 0 : 0 : 0 : 0 : 0 : 0)^T \end{aligned} \tag{5}$$

is called the *kinematic mapping* and maps each Euclidean displacement $\mathcal{D}$ to a point P on $S_6^2 \subset P^7$.

Given a displacement $\mathcal{D}$ as in Eq. (1), it is straightforward to compute the Study parameters x_i, y_i. One can use one of the following formulas to compute the Euler parameters x_i directly from the 3×3 proper orthogonal matrix $\mathbf{A} = (a_{ij})_{i,j=1,\ldots,3}$

$$\begin{aligned} x_0 : x_1 : x_2 : x_3 &= 1 + a_{11} + a_{22} + a_{33} : a_{32} - a_{23} : a_{13} \\ &\quad - a_{31} : a_{21} - a_{12}, \\ x_0 : x_1 : x_2 : x_3 &= a_{32} - a_{23} : 1 + a_{11} - a_{22} - a_{33} : a_{12} \\ &\quad + a_{21} : a_{31} + a_{13}, \\ x_0 : x_1 : x_2 : x_3 &= a_{13} - a_{31} : a_{12} + a_{21} : 1 - a_{11} + a_{22} \\ &\quad - a_{33} : a_{23} + a_{32}, \\ x_0 : x_1 : x_2 : x_3 &= a_{21} - a_{12} : a_{31} + a_{13} : a_{23} + a_{32} : 1 - a_{11} \\ &\quad - a_{22} + a_{33}. \end{aligned} \tag{6}$$

These formulas are already due to Study.[4] If $\mathbf{A}$ is nonsymmetric, we can always take the first proportion of Eq. (6). If $\mathbf{A}$ is symmetric, then it describes a rotation about an angle of π and the first formula fails. In this case, we can always resort to one of the three remaining proportions. It should be noted, that at least one of the four proportions in Eq. (6) is nonzero. The y_i are given by

$$\begin{aligned} y_0 &= -\frac{1}{2}(t_3 x_3 + t_2 x_2 + t_1 x_1), \\ y_1 &= -\frac{1}{2}(t_3 x_2 - t_2 x_3 - t_1 x_0), \\ y_2 &= -\frac{1}{2}(-t_3 x_1 + t_1 x_3 - t_2 x_0), \\ y_3 &= -\frac{1}{2}(-t_3 x_0 + t_2 x_1 - t_1 x_2). \end{aligned} \tag{7}$$

Remark 1. Planar displacements and spherical displacements are included in the model presented above. The kinematic image of spherical displacements is obtained from Eq. (2) by setting $y_i = 0$

$$\mathbf{M} := \begin{bmatrix} 1 & 0 & 0 & 0 \\ 0 & x_0^2 + x_1^2 - x_3^2 - x_2^2 & -2x_0x_3 + 2x_2x_1 & 2x_3x_1 + 2x_0x_2 \\ 0 & 2x_2x_1 + 2x_0x_3 & x_0^2 + x_2^2 - x_1^2 - x_3^2 & -2x_0x_1 + 2x_3x_2 \\ 0 & -2x_0x_2 + 2x_3x_1 & 2x_3x_2 + 2x_0x_1 & x_0^2 + x_3^2 - x_2^2 - x_1^2 \end{bmatrix}.$$

It should be noted that spherical displacements generate linear 3-spaces on S_6^2. Because we have ∞^3 points in the Euclidean three space, which can serve as centers for spherical displacements, there are ∞^3 3-spaces of this type on the Study-quadric. The kinematic image of planar displacements could be obtained by setting $y_0 = y_1 = x_2 = x_3 = 0$. The kinematic images of planar displacements also generate 3-spaces on S_6^2. Because there are ∞^3 planes in the Euclidean three space, we have ∞^3 3-spaces of this type on S_6^2.

Hyperplanes in P^7 are determined by linear equations in the point coordinates

$$\mathbf{u}^T \cdot \mathbf{x} = 0 \tag{8}$$

where $\mathbf{u}$ is a 8-tuple. The entries of $\mathbf{u}$ are called hyperplane coordinates, and $\mathbf{x}$ describes an arbitrary point X in P^7. The relation (8) determines the duality in P^7. The intersection of hyperplane with S_6^2 yields a five parametric set of displacements.

For the following, it will be important to have an understanding of the effect of coordinate transformations in the Cartesian space to the representation of displacements in the kinematic image space. Let $\mathbf{A}$ be a displacement having the image space coordinates $A(a_0 : a_1 : a_2 : a_3 : a_4 :$

https://doi.org/10.1017/S0263574707003530 Published online by Cambridge University Press

$a_5 : a_6 : a_7$)

$$\mathbf{A} = \frac{1}{\Delta}\begin{bmatrix} a_0^2+a_1^2+a_2^2+a_3^2 & 0 & 0 & 0 \\ 2(a_4a_1-a_5a_0-a_7a_2+a_6a_3) & a_0^2+a_1^2-a_2^2-a_3^2 & 2(a_1a_2-a_0a_3) & 2(a_1a_3+a_0a_2) \\ 2(a_4a_2-a_6a_0-a_5a_3+a_7a_1) & 2(a_1a_2+a_0a_3) & a_0^2-a_1^2+a_2^2-a_3^2 & 2(a_2a_3-a_0a_1) \\ 2(a_4a_3-a_7a_0-a_6a_1+a_5a_2) & 2(a_1a_3-a_0a_2) & 2(a_2a_3+a_0a_1) & a_0^2-a_1^2-a_2^2+a_3^2 \end{bmatrix}$$

where $\Delta_1 = a_0^2+a_1^2+a_2^2+a_3^2$. Furthermore, let $\mathbf{T}$ be a fixed transformation with image space coordinates $T(t_0 : t_1 : t_2 : t_3 : t_4 : t_5 : t_6 : t_7)$. A change of coordinates in the base system is represented by a left multiplication of the transformation matrix $\mathbf{A}$ with the coordinate transformation matrix $\mathbf{T}$. The Study parameters of this matrix product are

$$\mathbf{t}\circ\mathbf{a} = \Delta\begin{bmatrix} a_0t_0-a_1t_1-a_2t_2-a_3t_3 \\ a_0t_1+a_1t_0+t_2a_3-t_3a_2 \\ a_0t_2+a_2t_0+a_1t_3-a_3t_1 \\ a_0t_3+a_3t_0+a_2t_1-a_1t_2 \\ a_0t_4-a_1t_5-a_2t_6-a_3t_7+a_4t_0-a_5t_1-a_6t_2-a_7t_3 \\ a_0t_5+a_1t_4-a_2t_7+a_3t_6+a_4t_1+a_5t_0-a_6t_3+a_7t_2 \\ a_0t_6+a_1t_7+a_2t_4-a_3t_5+a_4t_2+a_5t_3+a_6t_0-a_7t_1 \\ a_0t_7-a_1t_6+a_2t_5+a_3t_4+a_4t_3-a_5t_2+a_6t_1+a_7t_0 \end{bmatrix} \tag{9}$$

where

$$\Delta = \frac{a_0t_0-a_1t_1-a_2t_2-a_3t_3}{\left(a_0^2+a_1^2+a_2^2+a_3^2\right)\left(t_0^2+t_1^2+t_2^2+t_3^2\right)}.$$

As the Study parameters are homogeneous, Δ can be omitted. It is possible to write Eq. (9) as a transformation matrix $\mathbf{T}_b$ in P^7 multiplied by the vector $\mathbf{a}$ as

$$\mathbf{t}\circ\mathbf{a} = \mathbf{T}_b\mathbf{a}$$

where

$$\mathbf{T}_b = \begin{bmatrix} t_0 & -t_1 & -t_2 & -t_3 & 0 & 0 & 0 & 0 \\ t_1 & t_0 & -t_3 & t_2 & 0 & 0 & 0 & 0 \\ t_2 & t_3 & t_0 & -t_1 & 0 & 0 & 0 & 0 \\ t_3 & -t_2 & t_1 & t_0 & 0 & 0 & 0 & 0 \\ t_4 & -t_5 & -t_6 & -t_7 & t_0 & -t_1 & -t_2 & -t_3 \\ t_5 & t_4 & -t_7 & t_6 & t_1 & t_0 & -t_3 & t_2 \\ t_6 & t_7 & t_4 & -t_5 & t_2 & t_3 & t_0 & -t_1 \\ t_7 & -t_6 & t_5 & t_4 & t_3 & -t_2 & t_1 & t_0 \end{bmatrix}. \tag{10}$$

A coordinate transformation in the moving frame is described by right multiplication $\mathbf{A}\cdot\mathbf{T}$. Performing the same procedure as before, one obtains the representation of this transformation in the kinematic image space as

$$\mathbf{a}\circ\mathbf{t} = \mathbf{T}_m\mathbf{a}$$

where

$$\mathbf{T}_m = \begin{bmatrix} t_0 & -t_1 & -t_2 & -t_3 & 0 & 0 & 0 & 0 \\ t_1 & t_0 & t_3 & -t_2 & 0 & 0 & 0 & 0 \\ t_2 & -t_3 & t_0 & t_1 & 0 & 0 & 0 & 0 \\ t_3 & t_2 & -t_1 & t_0 & 0 & 0 & 0 & 0 \\ t_4 & -t_5 & -t_6 & -t_7 & t_0 & -t_1 & -t_2 & -t_3 \\ t_5 & t_4 & t_7 & -t_6 & t_1 & t_0 & t_3 & -t_2 \\ t_6 & -t_7 & t_4 & t_5 & t_2 & -t_3 & t_0 & t_1 \\ t_7 & t_6 & -t_5 & t_4 & t_3 & t_2 & -t_1 & t_0 \end{bmatrix}. \tag{11}$$

The index m indicates the transformation in the moving frame. Summarizing the observations above yields:

Theorem 1. *Coordinate transformations in the base or moving frame of a manipulator can be written as projective transformations in the kinematic image space. The elements of the matrices describing these transformations are linear in only one of its Study parameters.*

1.1.1. Properties of $\mathbf{T}_b$ *and* $\mathbf{T}_m$.

Lemma 1. *The matrix product of* $\mathbf{T}_b$ *and* $\mathbf{T}_m$ *is commutative.*

Proof. We rewrite the matrices $\mathbf{T}_b$ and $\mathbf{T}_m$, using the 4×4 matrices $\mathbf{A}$, $\mathbf{B}$, $\mathbf{C}$, and $\mathbf{D}$

$$\mathbf{T_b} = \begin{bmatrix} \mathbf{A} & \mathbf{0} \\ \mathbf{B} & \mathbf{A} \end{bmatrix}, \qquad \mathbf{T_m} = \begin{bmatrix} \mathbf{C} & \mathbf{0} \\ \mathbf{D} & \mathbf{C} \end{bmatrix}.$$

Then, the products are

$$\mathbf{T}_b\cdot\mathbf{T}_m = \begin{bmatrix} \mathbf{AC} & \mathbf{0} \\ \mathbf{BC}+\mathbf{AD} & \mathbf{AC} \end{bmatrix},$$

$$\mathbf{T}_m\cdot\mathbf{T}_b = \begin{bmatrix} \mathbf{CA} & \mathbf{0} \\ \mathbf{DA}+\mathbf{CB} & \mathbf{CA} \end{bmatrix}.$$

The 4×4 submatrices $\mathbf{A}$, $\mathbf{B}$, $\mathbf{C}$, and $\mathbf{D}$ are well known in geometry. They describe the Clifford translations in an elliptic space (see Giering[8]). The commutativity of Clifford translations yields the commutativity of the product of $\mathbf{T}_b$ and $\mathbf{T}_m$. The same result can be obtained by direct computations. □

In other words, Lemma 1 expresses that it does not matter which coordinate transformation is performed first in the kinematic image space. This is what one would expect because of the same fact in the Euclidean space.

Lemma 2. *The inverse matrices* $\mathbf{T}_b^{-1}$ *and* $\mathbf{T}_m^{-1}$ *can be obtained by the substitution* $T\to\widetilde{T}$, $(t_0,t_1,t_2,t_3)\to(t_0,-t_1,-t_2,-t_3)$, *and* $(t_4,t_5,t_6,t_7)\to(t_5,-t_6,-t_7,-t_7)$ *in* $\mathbf{T}_b$ *resp.* $\mathbf{T}_m$.

Proof. Direct computation of $\mathbf{T}_b\cdot\widetilde{\mathbf{T}_b}$ (resp. $\mathbf{T}_m\cdot\widetilde{\mathbf{T}_m}$) yields a multiple of the unit matrix. Because of the homogeneity of the Study-parameters, this multiple can be omitted. □

Lemma 3. *The matrices* $\mathbf{T}_b$ *and* $\mathbf{T}_m$ *describe transformations in the kinematic image space that map points of* S_6^2 *onto points of* S_6^2. *Furthermore, the exceptional generator of this*

https://doi.org/10.1017/S0263574707003530 Published online by Cambridge University Press

quadric, defined by $x_0 = x_1 = x_2 = x_3 = 0$, is mapped onto itself and points of the quadric in this exceptional 3-space having the equation $y_0^2 + y_1^2 + y_2^2 + y_3^2 = 0$ are mapped onto points on the same quadric.

Proof. Because of the construction of the matrices $\mathbf{T}_b$ and $\mathbf{T}_m$, the transformed points $\mathbf{T}_b \cdot \mathbf{a}$ and $\mathbf{T}_m \cdot \mathbf{a}$ have to fulfill the equation of S_6^2. The second part of the lemma is also easy to see. Points in the exceptional generator have coordinates $(0 : 0 : 0 : 0 : y_0 : y_1 : y_2 : y_3)$. Because of the upper right 4×4 zero matrix in $\mathbf{T}_b$ and $\mathbf{T}_m$, the transformed point has to lie within this generator and has coordinates $(0 : 0 : 0 : 0 : \overline{y}_0 : \overline{y}_1 : \overline{y}_2 : \overline{y}_3)$. Substitution of these coordinates into the equation $y_0^2 + y_1^2 + y_2^2 + y_3^2 = 0$ yields $(y_1^2 + y_2^2 + y_3^2 + y_4^2)(t_0^2 + t_1^2 + t_2^2 + t_3^2) = 0$. Therefore, if the point lies on this quadric before the transformation, then it is contained in the quadric after the transformation. □

The transformations $\mathbf{T}_b$ and $\mathbf{T}_m$ are point transformations. In the following, the action of coordinate transformations in the Cartesian space on hyperplanes in the kinematic image space is derived.

Lemma 4. *Let* $\mathbf{T}$ *be a point transformation in* P^7 *and a point* $X \in P^7$ *described by* $\mathbf{x}$ *and*

$$X \to \widetilde{X} = \mathbf{T} \cdot \mathbf{x}.$$

This point transformation transforms the hyperplane with the equation

$$\mathbf{u}^T \cdot \mathbf{x} = 0$$

into the hyperplane

$$\widetilde{\mathbf{u}}^T \cdot \widetilde{\mathbf{x}} = 0$$

where $\widetilde{\mathbf{u}} = (\mathbf{T}^T)^{-1} \cdot \mathbf{u}$. *That means that* $(\mathbf{T}^T)^{-1}$ *is the corresponding transformation for the hyperplane coordinates* $\mathbf{u}$. *Furthermore* $\mathbf{T}$ *transforms a quadric described by the equation*

$$\mathbf{x}^T \cdot \mathbf{A} \cdot \mathbf{x} = 0$$

into the quadric

$$\widetilde{\mathbf{x}}^T \cdot \widetilde{\mathbf{A}} \cdot \widetilde{\mathbf{x}} = 0,$$

where $\widetilde{\mathbf{A}} = (\mathbf{T}^T)^{-1} \cdot \mathbf{A} \cdot \mathbf{T}^{-1}$.

Proof. If $\mathbf{u}^T \cdot \mathbf{x} = 0$ and $X \to \widetilde{X} = \mathbf{T} \cdot \mathbf{x}$, then one has to look for a $\widetilde{\mathbf{u}}$ such that $\widetilde{\mathbf{u}}^T \cdot \widetilde{\mathbf{x}} = \widetilde{\mathbf{u}}^T \cdot \mathbf{T} \cdot \mathbf{x} = 0$. This implies $\mathbf{u}^T = \widetilde{\mathbf{u}}^T \cdot \mathbf{T}$ or $\widetilde{\mathbf{u}} = (\mathbf{T}^T)^{-1}\mathbf{u}$.

If $\mathbf{x}^T \cdot \mathbf{A} \cdot \mathbf{x} = 0$ and $X \to \widetilde{X} = \mathbf{T} \cdot \mathbf{x}$, then one has to look for a $\widetilde{\mathbf{A}}$ such that $\widetilde{\mathbf{x}}^T \cdot \widetilde{\mathbf{A}} \cdot \widetilde{\mathbf{x}} = (\mathbf{T} \cdot \mathbf{x})^T \cdot \widetilde{\mathbf{A}} \cdot \mathbf{T} \cdot \mathbf{x} = \mathbf{x}^T \cdot \mathbf{T}^T \cdot \widetilde{\mathbf{A}} \cdot \mathbf{T} \cdot \mathbf{x}$. This implies that $\mathbf{A} = \mathbf{T}^T \cdot \widetilde{\mathbf{A}} \cdot \mathbf{T}$ or $\widetilde{\mathbf{A}} = (\mathbf{T}^T)^{-1} \cdot \widetilde{\mathbf{A}} \cdot \mathbf{T}^{-1}$. □

1.2. Constraint varieties for mechanism analysis and synthesis

The basic idea to analyze mechanisms with kinematic mapping is the following: every mechanism generates a certain set of points, curves, surfaces, or higher dimensional objects of up to five dimensions in the image space. Generally, the dimension of the object corresponds to the degree of freedom of the mechanism. If, for example, one point of the moving system of a spatial mechanical device is bound to move on a surface, the system still has five degrees of freedom. Therefore, the mechanical constraint is mapped to a hypersurface in kinematic image space. From this statement, we can conclude that every mechanical system in general can be described by a system of equations. If the constraints are of algebraic nature, then the equations are algebraic (polynomials). Revolute joints, for example, are algebraic constraints. The condition that one point of the moving system is bound to move on a circle or on a sphere are algebraic constraints. For the following, we restrict the constraints to algebraic ones.

From the algebraic point of view, we have then a system of polynomial equations $I = (g_1, \ldots, g_n)$, which corresponds to an algebraic variety $V = V(g_1, \ldots, g_n)$. The algebraic varieties are the constraint surfaces. With this interpretation it is possible to use all the progress, which was made in recent years, in solving systems of polynomial equations (see Dickenstein and Emiris[2]).

We show this idea with a simple example (see Husty[9]): consider a planar parallel manipulator consisting of a base and a platform linked by three RPR-legs (Fig. 1). In the direct kinematics, we are given the design of the manipulator, i.e., the design of base and platform (the coordinates B_1, C_1, C_2, a_1, a_2, b_1, b_2, c_1, c_2 and the lengths of the legs r_1, r_2, r_3). The task is to find all assembly modes.

Geometric preprocessing transforms the direct kinematics problem now into the following task: given a triangle and three circles, place the triangle such that its three vertices are on the circles (vertex A on circle k_1, etc., Fig. 2). The circles constitute now the mechanical constraints. If, for a moment, we just consider one circle, then we can say, for example, that mechanically point A is constrained to move on circle k_1. Using planar kinematic mapping, this constraint is mapped to a hypersurface in the three-dimensional kinematic

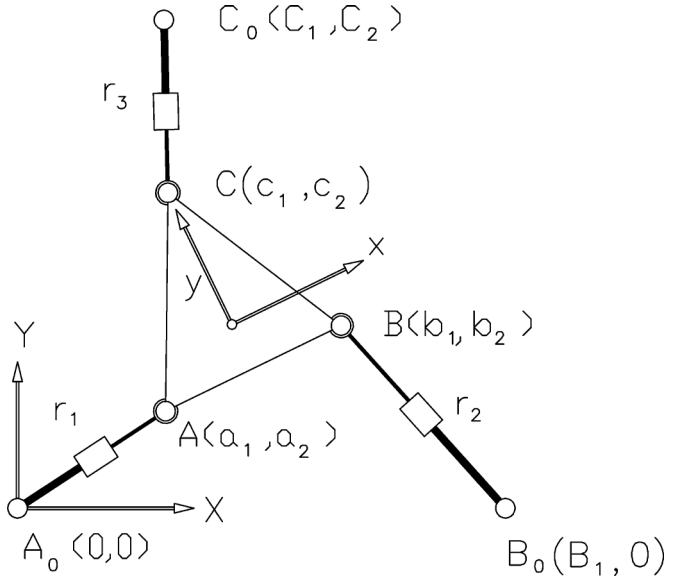

Fig. 1. 3RPR-platform.

https://doi.org/10.1017/S0263574707003530 Published online by Cambridge University Press

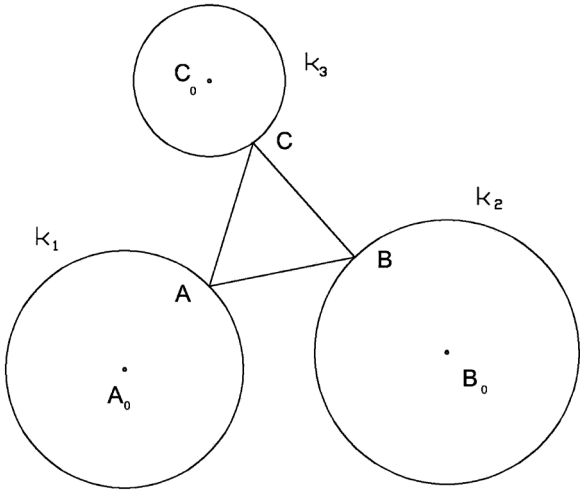

Fig. 2. Geometric equivalent.

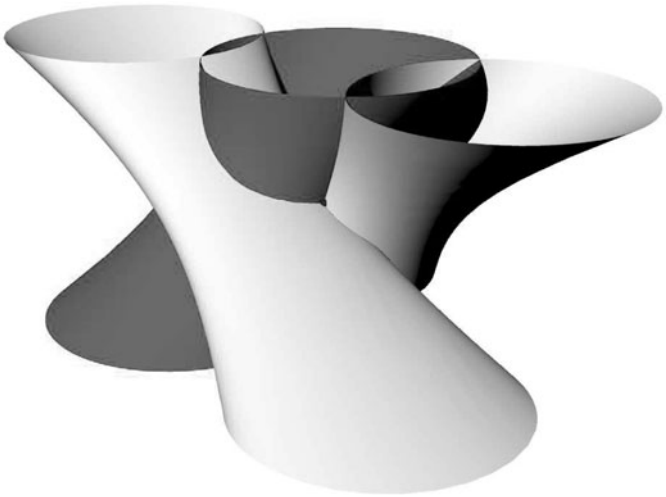

Fig. 3. Constraint surfaces in kinematic image space.

image space. It turns out that the constraint surface is a special hyperboloid in this space (Fig. 3).[10] Algebraically, this hypersurface for the point C is given by

$$h_1 : \left(y_2 - \frac{1}{2}(c_2 + C_2 - x_1(C_1 - c_1))\right)^2 + \left(y_3 - \frac{1}{2}(x_1(c_2 - C_2) - C_1 - c_1)\right)^2 - \frac{1}{4}r_3^2\left(x_1^2 + 1\right) = 0. \tag{12}$$

From the algebraic point of view, we have three quadratic polynomials h_1, h_2, h_3, which determine the algebraic variety $V = V(h_1, h_2, h_3)$. The dimension of this variety is zero; it consists of eight points. Six of these points are solutions to the direct kinematics problem, two of the points are always complex and do not solve the task (see Husty[9]) or Brunnthaler *et al.*[11]).

2. Application to Mechanism Analysis

In this section, we show how the above developed theory is applied to mechanism analysis. We point out how the representation of coordinate transformations in the image space helps to simplify the inverse kinematic algorithm presented in Husty *et al.*[12,13]. Furthermore, we reveal how the jump of the dimension of the algebraic solution varieties determines overconstrained $6R$ chains.

It should be noted that this approach was already successfully applied to the analysis of parallel mechanisms to derive the direct kinematics, and to determine architecturally singular and pathologically movable platform mechanisms.[14–16]

2.1. Kinematic image of a 3R serial chain

To solve the inverse kinematics of a general $6R$, we will split the $6R$ into two $3R$ chains. Therefore, it will be important to derive the kinematic image of $3R$ chains. The advantage of the transformations developed in Section 1.1 is that we only have to derive the corresponding variety in a canonical form. This means that we can place the $3R$ chain in the Cartesian space in the most suitable way and perform the coordinate transformation to a general position in the kinematic image space. This procedure simplifies the necessary computations such that it is possible to write the equations of the constraint manifolds completely generally, i.e., without specifying the design parameters.

If the relative position of two rotation axes is described by the usual Denavit–Hartenberg parameters[17] (α_i, a_i, d_i), then the coordinate transformation between the coordinate systems attached to the rotation axes is given by

$$\mathbf{G} = \begin{bmatrix} 1 & 0 & 0 & 0 \\ a_i & 1 & 0 & 0 \\ 0 & 0 & \cos\alpha_i & -\sin\alpha_i \\ d_i & 0 & \sin\alpha_i & \cos\alpha_i \end{bmatrix}. \tag{13}$$

Using this transformation, we assume the axes of an nR-chain being in a canonical start position, where all the axes are parallel to a plane, the first rotation axis is the z-axis of the base coordinate system and the x-axis is the common normal of first and second rotation axis. A simple consideration shows that this is always possible, and there is no restriction of generality.[18] As shown in Fig. 4, the rotation axes are always the z-axes of the coordinate systems. Therefore, we can write these rotations as

$$\mathbf{M}_i = \begin{bmatrix} 1 & 0 & 0 & 0 \\ 0 & \cos u_i & -\sin u_i & 0 \\ 0 & \sin u_i & \cos u_i & 0 \\ 0 & 0 & 0 & 1 \end{bmatrix} \tag{14}$$

with u_i being the rotation parameters. The forward kinematics of a general $3R$ chain can be written as

$$\mathbf{D} = \mathbf{B} \cdot \mathbf{M}_1 \cdot \mathbf{G}_1 \cdot \mathbf{M}_2 \cdot \mathbf{G}_2 \cdot \mathbf{M}_3 \cdot \mathbf{G}_3.$$

The constant matrix $\mathbf{B}$ performs the transformation of an arbitrary coordinate system into the canonical base system of Fig. 4.

In a step by step procedure, the representation of the $3R$ in the image space will be derived. At first, we will derive

https://doi.org/10.1017/S0263574707003530 Published online by Cambridge University Press

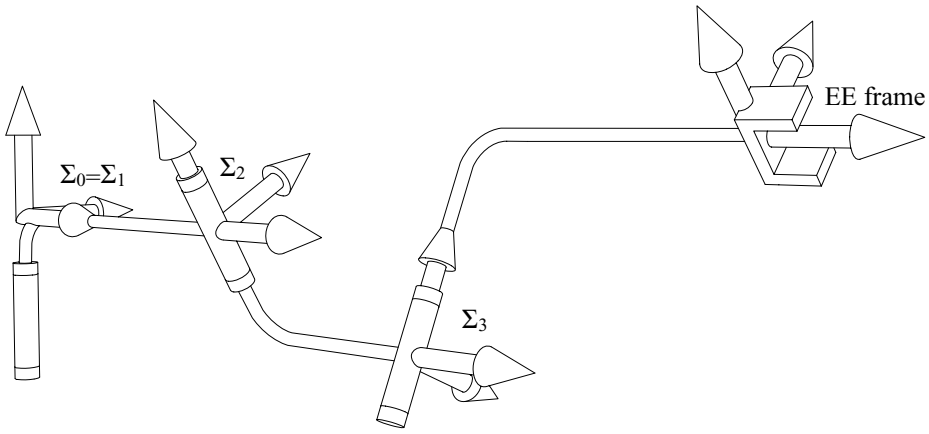

Fig. 4. Canonical $3R$-manipulator.

the representation for the canonical chain for which **B** is the identity. The transformation that brings the chain into a general position will be performed later in the image space.

If one of the three rotation parameters of the $3R$ chain is fixed for a moment, then a $2R$ chain remains. The kinematic image of this $2R$ chain is derived first. We have three possibilities to fix a rotation parameter. The procedure is slightly different for each of the three possibilities. We demonstrate the computation for the parameter u_1. The other two possibilities can be found in the work of Pfurner.[18]

Fixing the first revolute axis $u_1 = u_{10}$ (the zero in the index indicates a fixed value), the corresponding $2R$ chain has the matrix representation

$$\mathbf{D} = \mathbf{F} \cdot \mathbf{M}_2 \cdot \mathbf{G}_2 \cdot \mathbf{M}_3 \cdot \mathbf{G}_3$$

where **F** is a fixed transformation, given by $\mathbf{M}_1(u_{10}) \cdot \mathbf{G}_1$. **F** and $\mathbf{G}_3$ are coordinate transformations in the base respectively moving frame of this $2R$ chain. Neglecting **F** and setting $d_2 = 0$ transforms the chain into a canonical one as shown in Fig. 5. Setting $d_2 = 0$ means no loss of generality, because a transformation in the direction of the second revolute axis can be achieved later directly in the kinematic image space. Omitting $\mathbf{G}_3$ transforms the end effector frame such that the z-axis coincides with the second axis of this $2R$ chain, and the x-axis is aligned with the common normal of the two revolute axes.

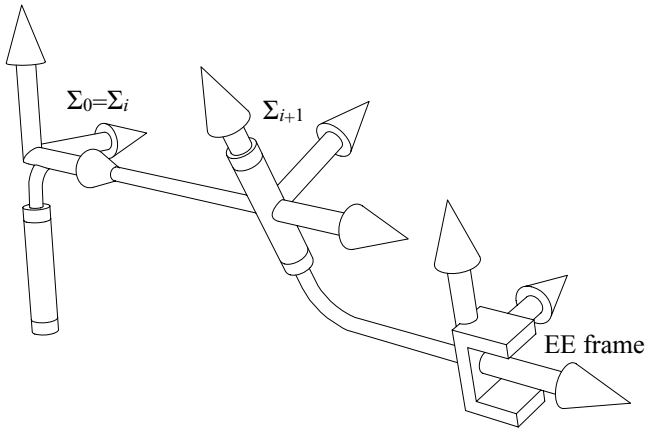

Fig. 5. Canonical $2R$-mechanism.

Then, the matrix representation of the remaining $2R$ chain becomes

$$\mathbf{D} = \mathbf{M}_2 \cdot \mathbf{G}_2 \cdot \mathbf{M}_3. \tag{15}$$

The parametric representation of the constraint manifold, computed with Eqs. (6) and (7) reads

$$\begin{bmatrix} x_0 \\ x_1 \\ x_2 \\ x_3 \\ y_0 \\ y_1 \\ y_2 \\ y_3 \end{bmatrix} = \begin{bmatrix} (\cos u_2 \cos u_3 - \sin u_2 \sin u_3 + 1)(1 + \cos \alpha_2) \\ (\cos u_2 + \cos u_3) \sin \alpha_2 \\ (\sin u_2 - \sin u_3) \sin \alpha_2 \\ (\cos u_2 \sin u_3 + \sin u_2 \cos u_3)(1 + \cos \alpha_2) \\ \frac{1}{2} a_2 (\cos u_2 \cos u_3 - \sin u_2 \sin u_3 + 1)(\sin \alpha_2) \\ -\frac{1}{2} a_2 (\cos u_2 + \cos u_3)(1 + \cos \alpha_2) \\ -\frac{1}{2} a_2 (\sin u_2 - \sin u_3)(1 + \cos \alpha_2) \\ \frac{1}{2} a_2 (\cos u_2 \sin u_3 + \sin u_2 \cos u_3)(\sin \alpha_2) \end{bmatrix}.$$

By inspection and direct substitution one can verify easily that these coordinates satisfy four independent linear equations

$$\begin{aligned} \overline{Hc}_{11} &: a_2 \sin \alpha_2 x_0 - 2(1 + \cos \alpha_2) y_0 = 0, \\ \overline{Hc}_{12} &: a_2 (1 + \cos \alpha_2) x_1 + 2 \sin \alpha_2 y_1 = 0, \\ \overline{Hc}_{13} &: a_2 (1 + \cos \alpha_2) x_2 + 2 \sin \alpha_2 y_2 = 0, \\ \overline{Hc}_{14} &: a_2 \sin \alpha_2 x_3 - 2(1 + \cos \alpha_2) y_3 = 0. \end{aligned}$$

Applying half tangent substitution ($al_2 = \tan \alpha_2/2$), these equations rewrite to

$$\begin{aligned} \overline{Hc}_{11} &: a_2 al_2 x_0 - 2 y_0 = 0, \\ \overline{Hc}_{12} &: a_2 x_1 + 2 al_2 y_1 = 0, \\ \overline{Hc}_{13} &: a_2 x_2 + 2 al_2 y_2 = 0, \\ \overline{Hc}_{14} &: a_2 al_2 x_3 - 2 y_3 = 0. \end{aligned} \tag{16}$$

Similar equations have been derived by Selig.[7]

https://doi.org/10.1017/S0263574707003530 Published online by Cambridge University Press

In the next step, we add the rotation about the first axis having the parameter u_1 and a constant transformation in the moving frame to transform it into a general position. In this case, one has to apply the (now one parametric set of) coordinate transformations $\mathbf{M}_1 \cdot \mathbf{G}_1 \cdot \overline{\mathbf{G}}_2$ in the base frame and $\mathbf{G}_3$ in the moving frame of the $2R$ chain. $\overline{\mathbf{G}}_2$ translates the base frame by d_2 in the direction of the z-axis (same matrix as $\mathbf{G}_2$ but $a_2 = 0$, $\alpha_2 = 0$). This is the new and essential contribution of this work that the transformations bringing the canonical manifolds to a general position can be performed efficiently in the kinematic image space. Although the theory seems to be a bit complicated, its application makes the necessary computation simple.

The necessary transformations are executed directly on the hyperplanes of Eq. (16), which describe the canonical $2R$ chain in the kinematic image space. The point transformation in the base frame would be $\mathbf{T}_b(\mathbf{M}_1) \cdot \mathbf{T}_b(\mathbf{G}_1) \cdot \mathbf{T}_b(\overline{\mathbf{G}}_2)$, so according to Lemma 4, the hyperplane transformation is $((\mathbf{T}_b(\mathbf{M}_1) \cdot \mathbf{T}_b(\mathbf{G}_1) \cdot \mathbf{T}_b(\overline{\mathbf{G}}_2))^T)^{-1} = (\mathbf{T}_b(\mathbf{M}_1)^T)^{-1} \cdot (\mathbf{T}_b(\mathbf{G}_1)^T)^{-1} \cdot (\mathbf{T}_b(\overline{\mathbf{G}}_2)^T)^{-1}$. After applying the half tangent substitutions for all angles ($v_1 = \tan\frac{u_1}{2}$, $al_i = \tan\frac{\alpha_i}{2}$, $i = 1, 2$), these transformations can be written as

$$(\mathbf{T}_b(\mathbf{M}_1)^T)^{-1} = \begin{bmatrix} 1 & 0 & 0 & -v_1 & 0 & 0 & 0 & 0 \\ 0 & 1 & -v_1 & 0 & 0 & 0 & 0 & 0 \\ 0 & v_1 & 1 & 0 & 0 & 0 & 0 & 0 \\ v_1 & 0 & 0 & 1 & 0 & 0 & 0 & 0 \\ 0 & 0 & 0 & 0 & 1 & 0 & 0 & -v_1 \\ 0 & 0 & 0 & 0 & 0 & 1 & -v_1 & 0 \\ 0 & 0 & 0 & 0 & 0 & v_1 & 1 & 0 \\ 0 & 0 & 0 & 0 & v_1 & 0 & 0 & 1 \end{bmatrix},$$

$$(\mathbf{T}_b(\mathbf{G}_1)^T)^{-1} = \begin{bmatrix} 2 & -2al_1 & 0 & 0 & al_1a_1 & a_1 & al_1 & 0 \\ 2al_1 & 2 & 0 & 0 & -a_1 & al_1a_1 & 0 & -al_1 \\ 0 & 0 & 2 & -2al_1 & -al_1 & 0 & al_1a_1 & a_1 \\ 0 & 0 & 2al_1 & 2 & 0 & al_1 & -a_1 & al_1a_1 \\ 0 & 0 & 0 & 0 & 2 & -2al_1 & 0 & 0 \\ 0 & 0 & 0 & 0 & 2al_1 & 2 & 0 & 0 \\ 0 & 0 & 0 & 0 & 0 & 0 & 2 & -2al_1 \\ 0 & 0 & 0 & 0 & 0 & 0 & 2al_1 & 2 \end{bmatrix},$$

$$(\mathbf{T}_b(\overline{\mathbf{G}}_2)^T)^{-1} = \begin{bmatrix} 2 & 0 & 0 & 0 & 0 & 0 & 0 & d_2 \\ 0 & 2 & 0 & 0 & 0 & 0 & d_2 & 0 \\ 0 & 0 & 2 & 0 & 0 & -d_2 & 0 & 0 \\ 0 & 0 & 0 & 2 & -d_2 & 0 & 0 & 0 \\ 0 & 0 & 0 & 0 & 2 & 0 & 0 & 0 \\ 0 & 0 & 0 & 0 & 0 & 2 & 0 & 0 \\ 0 & 0 & 0 & 0 & 0 & 0 & 2 & 0 \\ 0 & 0 & 0 & 0 & 0 & 0 & 0 & 2 \end{bmatrix}.$$

The coordinate transformation $\mathbf{G}_3$ in E^3 of the moving frame can be performed with the help of

$$(\mathbf{T}_m(\mathbf{G}_3)^T)^{-1} = \begin{bmatrix} 2 & -2al_3 & 0 & 0 & al_3a_3 & a_3 & al_3d_3 & d_3 \\ 2al_3 & 2 & 0 & 0 & -a_3 & al_3a_3 & -d_3 & al_3d_3 \\ 0 & 0 & 2 & 2al_3 & -al_3d_3 & d_3 & al_3a_3 & -a_3 \\ 0 & 0 & -2al_3 & 2 & -d_3 & -al_3d_3 & a_3 & al_3a_3 \\ 0 & 0 & 0 & 0 & 2 & -2al_3 & 0 & 0 \\ 0 & 0 & 0 & 0 & 2al_3 & 2 & 0 & 0 \\ 0 & 0 & 0 & 0 & 0 & 0 & 2 & 2al_3 \\ 0 & 0 & 0 & 0 & 0 & 0 & -2al_3 & 2 \end{bmatrix}$$

where $al_3 = \tan\frac{\alpha_3}{2}$ in P^7. Applying all transformations of the base and moving frames on the hyperplane coordinates of the hyperplanes in Eq. (16) yields the four linear equations

$$\begin{aligned} &Hc_1(v_1): \\ &(a_2al_2 - v_1d_2 - al_3a_1 - al_3a_3 - al_1a_1 - a_2al_2al_3al_1 \\ &\quad - al_3v_1d_2al_1 - al_3d_3al_1v_1 - a_3al_1 - d_3v_1)x_0 \\ &\quad + (-al_3v_1d_2 + a_2al_2al_3 + a_2al_2al_1 + a_1 + a_3 - al_3al_1a_1 \\ &\quad + v_1d_2al_1 - al_3a_3al_1 + d_3al_1v_1 - al_3d_3v_1)x_1 + (a_1v_1 \\ &\quad - d_2al_1 + al_3d_3 - d_3al_1 + a_2al_2al_1v_1 + al_3d_2 \\ &\quad - al_3al_1a_1v_1 - al_3a_3al_1v_1 + a_3v_1 + a_2al_2al_3v_1)x_2 \\ &\quad + (-a_3al_1v_1 + d_2 + d_3 - al_1a_1v_1 + a_2al_2v_1 - al_3a_1v_1 \\ &\quad + al_3d_2al_1 + al_3d_3al_1 - a_2al_2al_3al_1v_1 - al_3a_3v_1)x_3 \\ &\quad + 2(al_3al_1 - 1)y_0 - 2(al_3 + al_1)y_1 - 2(al_1v_1 + al_3v_1)y_2 \\ &\quad + 2(al_3al_1v_1 - v_1)y_3 = 0. \end{aligned} \tag{17}$$

$$\begin{aligned} &Hc_2(v_1): \\ &(al_2a_1 + al_2v_1d_2al_1 - a_2al_1 - al_2al_3al_1a_1 - al_2al_3a_3al_1 \\ &\quad - al_2al_3v_1d_2 - al_2d_3al_1v_1 - a_2al_3 + al_2a_3 + al_2al_3d_3v_1)x_0 \\ &\quad + (-a_2al_3al_1 + al_2v_1d_2 - al_2al_3d_3al_1v_1 + al_2al_3a_1 \\ &\quad + al_2al_3a_3 - al_2d_3v_1 + al_2al_1a_1 + al_2a_3al_1 + a_2 \\ &\quad + al_2al_3v_1d_2al_1)x_1 + (al_2d_3 - al_2d_2 + al_2al_3a_1v_1 \\ &\quad - al_2al_3d_2al_1 - a_2al_3al_1v_1 + al_2al_1a_1v_1 + al_2al_3a_3v_1 \\ &\quad + al_2a_3al_1v_1 + al_2al_3d_3al_1 + a_2v_1)x_2 + (al_2a_1v_1 \\ &\quad - a_2al_3v_1 - al_2d_2al_1 + al_2al_3d_2 - al_2al_3d_3 + al_2a_3v_1 \\ &\quad + al_2d_3al_1 - al_2al_3al_1a_1v_1 - al_2al_3a_3al_1v_1 - a_2al_1v_1)x_3 \\ &\quad - 2(al_2al_3 + al_2al_1)y_0 + 2(-al_2al_3al_1 + al_2)y_1 \\ &\quad + 2(al_2v_1 - al_2al_3al_1v_1)y_2 - 2(al_2al_3v_1 + al_2al_1v_1)y_3 = 0. \end{aligned} \tag{18}$$

https://doi.org/10.1017/S0263574707003530 Published online by Cambridge University Press

$$
\begin{aligned}
&Hc_3(v_1):\\
&(-al_2a_3v_1 + al_2al_3d_3 + al_2a_1v_1 - al_2d_2al_1 - al_2al_3d_2\\
&\quad + al_2al_3al_1a_1v_1 - al_2al_3a_3al_1v_1 + al_2d_3al_1 - a_2al_1v_1\\
&\quad + a_2al_3v_1)x_0 + (-al_2al_3a_3v_1 + al_2al_3d_3al_1 - a_2v_1\\
&\quad + al_2d_2 - al_2d_3 - a_2al_3al_1v_1 + al_2al_3a_1v_1 - al_2al_3d_2al_1\\
&\quad - al_2al_1a_1v_1 + al_2a_3al_1v_1)x_1 + (a_2al_3al_1 + a_2\\
&\quad - al_2al_3v_1d_2al_1 + al_2v_1d_2 + al_2al_1a_1 + al_2al_3d_3al_1v_1\\
&\quad - al_2d_3v_1 + al_2al_3a_3 - al_2a_3al_1 - al_2al_3a_1)x_2 + (a_2al_1\\
&\quad - al_2a_1 + al_2a_3 - al_2al_3v_1d_2 - al_2al_3al_1a_1 - al_2v_1d_2al_1\\
&\quad + al_2d_3al_1v_1 + al_2al_3d_3v_1 - a_2al_3 + al_2al_3a_3al_1)x_3\\
&\quad + 2(al_2al_3v_1 - al_2al_1v_1)y_0 - 2(al_2v_1 + al_2al_3al_1v_1)y_1\\
&\quad + 2(al_2al_3al_1 + al_2)y_2 + 2(-al_2al_3\\
&\quad + al_2al_1)y_3 = 0. \qquad (19)
\end{aligned}
$$

$$
\begin{aligned}
&Hc_4(v_1):\\
&(-d_2 + al_3a_3v_1 - d_3 - a_3al_1v_1 + al_3d_3al_1 - a_2al_2al_3al_1v_1\\
&\quad - a_2al_2v_1 + al_1a_1v_1 - al_3a_1v_1 + al_3d_2al_1)x_0 + (a_1v_1\\
&\quad - d_2al_1 - al_3d_2 - a_2al_2al_3v_1 + a_2al_2al_1v_1 + al_3al_1a_1v_1\\
&\quad - al_3a_3al_1v_1 - a_3v_1 - d_3al_1 - al_3d_3)x_1 + (a_2al_2al_3\\
&\quad + al_3a_3al_1 - v_1d_2al_1 - d_3al_1v_1 - a_2al_2al_1 - a_1 + a_3\\
&\quad - al_3v_1d_2 - al_3al_1a_1 - al_3d_3v_1)x_2 + (a_2al_2 + a_3al_1\\
&\quad - al_3a_3 - al_1a_1 + al_3a_1 - d_3v_1 + a_2al_2al_3al_1\\
&\quad + al_3v_1d_2al_1 + al_3d_3al_1v_1 - v_1d_2)x_3 + 2(al_3al_1v_1\\
&\quad + v_1)y_0 + 2(al_3v_1 - al_1v_1)y_1 + 2(al_1 - al_3)y_2\\
&\quad + -2(1 + al_3al_1)y_3 = 0. \qquad (20)
\end{aligned}
$$

Each of the hyperplanes Hc_i depends on the parameter v_1. Intersecting this set of hyperplane equations yields a one parameter set of 3-spaces $T_c(v_1)$ whose intersection with the Study quadric is the constraint manifold of the canonical serial $3R$ chain.

Remark 2. It has to be emphasized that the presented algorithm allows one to write the equations completely generally, i.e., without specifying the Denavit–Hartenberg parameters.

Remark 3. Almost the same procedure can be done with the other two possibilities. One can fix u_2 or u_3 and obtain in each case a one parameter set of 3-spaces $T_c(v_2)$ and $T_c(v_3)$ with v_2 and v_3 being the algebraic values of u_2 and u_3. It should be noted that the intersection of each of these sets of 3-spaces and S_6^2 yields the same constraint manifold. The two other possibilities just provide a redundant description of the constraint manifold. It is advantageous to have this description to handle all special cases that can occur (see next remark).

Remark 4. The intersection of $T_c(v_1)$ and S_6^2 fails if $T_c(v_1)$ lies on S_6^2. This happens when the second and the third revolute axes are parallel or intersect. In this cases, one has to take another set of hyperplane equations $T_c(v_2)$ or $T_c(v_3)$ to compute the constraint manifold.

Remark 5. If the $3R$ chain is planar or spherical, the equations of the hyperplanes simplify considerablly. In the planar case we have

$$
\begin{aligned}
&Hc_{p1}: \; -al_3x_0 + x_1 = 0,\\
&Hc_{p2}: \; x_2 - al_3x_3 = 0,\\
&Hc_{p3}: \; al_3a_3x_0 - a_3x_1 - al_3d_3x_2 - d_3x_3\\
&\qquad +2y_0 + 2al_3y_1 = 0,\\
&Hc_{p4}: \; d_3x_0 + al_3d_3x_1 - a_3x_2 + al_3a_3x_3\\
&\qquad + 2al_3y_2 + 2y_3 = 0.
\end{aligned} \qquad (21)
$$

And in the spherical case, the equations are

$$
\begin{aligned}
&Hc_{w1}: \; al_3a_3x_0 - a_3x_1 - al_3d_3x_2 - d_3x_3\\
&\qquad + 2y_0 + 2al_3y_1 = 0,\\
&Hc_{w2}: \; a_3x_0 + al_3a_3x_1 + d_3x_2 - al_3d_3x_3\\
&\qquad - 2al_3y_0 + 2y_1 = 0,\\
&Hc_{w3}: \; al_3d_3x_0 - d_3x_1 + al_3a_3x_2 + a_3x_3\\
&\qquad + 2y_2 - 2al_3y_3 = 0,\\
&Hc_{w4}: \; d_3x_0 + al_3d_3x_1 - a_3x_2 + al_3a_3x_3\\
&\qquad + 2al_3y_2 + 2y_3 = 0.
\end{aligned} \qquad (22)
$$

The last step is now to introduce the general case. It differs from the canonical $3R$ chains by having a general position of the first revolute axis with respect to the fixed coordinate system (see Fig. 6).

Up to now, the $3R$ chain was always a canonical one, which means that the first axis is coincident with the z-axis of the base frame, and the Denavit–Hartenberg parameter d_2 is equal to zero. To derive from the constraint manifold of the canonical $3R$ chain the equations of the constraint manifold of an arbitrarily placed $3R$ chain, only a fixed coordinate transformation in the base frame is needed. This can be executed directly in the kinematic image space via the matrix $(\mathbf{T}_b^T)^{-1}$ (Eq. 10), applied to the one parameter sets of 3-spaces $T_c(v_1)$, $T_c(v_2)$, and $T_c(v_3)$, generated as intersections of the one parameter sets of hyperplanes in Eqs. (17)–(20), resp. the hyperplane equations of $T_c(v_2)$ and $T_c(v_3)$. We also have to apply this transformation to the fixed 3-spaces T_{cp} and T_{cw}, generated as the intersections of the hyperplanes in Eqs. (21) and (22). This procedure yields new sets of hyperplane equations intersecting in one parameter sets of 3-spaces resp. fixed 3-spaces. The resulting one parameter sets of 3-spaces will be denoted by $T(v_1)$, $T(v_2)$, and $T(v_3)$. The hyperplane equations describing these sets of 3-spaces are a little bit more complicated. Because of limit of space they are not displayed here. They consist of approximately 200 terms, and it should be noted that they still can be computed

https://doi.org/10.1017/S0263574707003530 Published online by Cambridge University Press

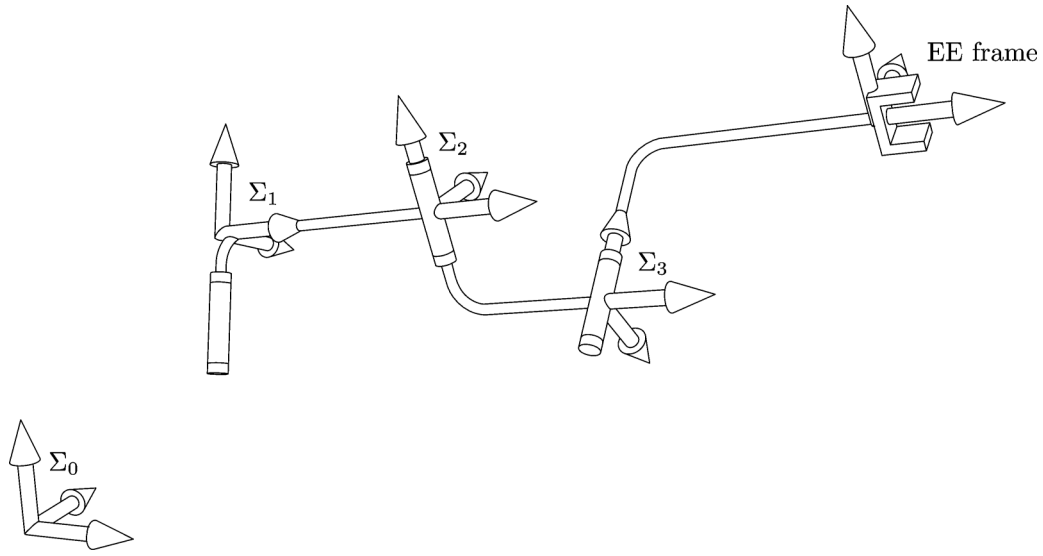

Fig. 6. General $3R$ serial chain.

completely generally, i.e., without specifying the Denavit–Hartenberg parameters. A complete listing of the general equations can be found in Pfurner.[18]

The hyperplane equations describing the fixed 3-space as the constraint manifold T_p of an arbitrary planar $3R$ mechanism, where the first axis does not coincide with the z-axis of the base frame, are

$$
\begin{aligned}
H_{p1}: \quad & -2x_0(t_0 al_3 + t_1) + 2x_1(-t_1 al_3 + t_0) \\
& + 2x_2(-t_2 al_3 + t_3) - 2x_3(t_3 al_3 + t_2) = 0, \\
H_{p2}: \quad & 2x_0(-t_2 + t_3 al_3) - 2x_1(t_3 + t_2 al_3) + 2x_2(t_0 + t_1 al_3) \\
& + 2x_3(t_1 - t_0 al_3) = 0, \\
H_{p3}: \quad & x_0(t_0 al_3 a_3 + t_1 a_3 + t_2 al_3 d_3 + t_3 d_3 + 2t_4 - 2t_5 al_3) \\
& + x_1(t_1 al_3 a_3 - t_0 a_3 + t_3 al_3 d_3 - t_2 d_3 + 2t_5 + 2t_4 al_3) \\
& + x_2(t_2 al_3 a_3 - t_3 a_3 - t_0 al_3 d_3 + t_1 d_3 + 2t_6 + 2t_7 al_3) \\
& + x_3(t_3 al_3 a_3 + t_2 a_3 - t_1 al_3 d_3 - t_0 d_3 + 2t_7 - 2t_6 al_3) \\
& + 2y_0(-t_1 al_3 + t_0) + 2y_1(t_1 + t_0 al_3) \\
& + 2y_2(t_2 + t_3 al_3) + 2y_3(t_3 - t_2 al_3) = 0, \\
H_{p4}: \quad & x_0(t_0 d_3 - t_1 al_3 d_3 + t_2 a_3 - t_3 al_3 a_3 - 2t_6 al_3 - 2t_7) \\
& + x_1(t_1 d_3 + t_0 al_3 d_3 + t_3 a_3 + t_2 al_3 a_3 - 2t_7 al_3 + 2t_6) \\
& + x_2(t_2 d_3 + t_3 al_3 d_3 - t_0 a_3 - t_1 al_3 a_3 + 2t_4 al_3 - 2t_5) \\
& + x_3(t_3 d_3 - t_2 al_3 d_3 - t_1 a_3 + t_0 al_3 a_3 + 2t_5 al_3 + 2t_4) \\
& - 2y_0(t_3 + t_2 al_3) + 2y_1(t_2 - t_3 al_3) + 2y_2(t_0 al_3 - t_1) \\
& + 2y_3(t_0 + t_1 al_3) = 0. \qquad (23)
\end{aligned}
$$

The remarkable result of this section is that we have found a completely general description of all possible $3R$ chains. The equations do not have to be computed once more for different designs. The design parameters can be substituted directly into the four hyperplane equations. Additionally, we have a redundant description of the generated one parameter sets of 3-spaces; so one only has to be aware about the layout of the chain to take the appropriate set of equations. This process can be fully automated.

2.2. *Properties of the constraint manifolds*

To pass from the constraint manifolds of a canonical $3R$ chain to those of a general arbitrary $3R$ chain, only a fixed coordinate transformation in the base frame was applied. It is important to observe that this transformation does not change the geometric shape and geometric properties of the manifold, but only the position in the kinematic image space. Therefore, the geometric properties for the manifolds $T(v_i)$ can be derived directly from $T_c(v_i)$, $i = 1, 2, 3$. The transformation from canonical form to general position will not change the geometric properties.

The one parameter sets of 3-spaces $T(v_1)$, $T(v_2)$, and $T(v_3)$ are well known in geometry. Geometrically, they can be obtained by the following algorithm: Take two 3-spaces in P^7 and define a linear relation between the points in these spaces, which means that each point of one space is joined by a line with exactly one corresponding point of the other three space. The manifold of all these lines is called a *Segre manifold*. A symbolic sketch of a Segre manifold is depicted in Fig. 7. In this figure, 3-spaces corresponding to discrete

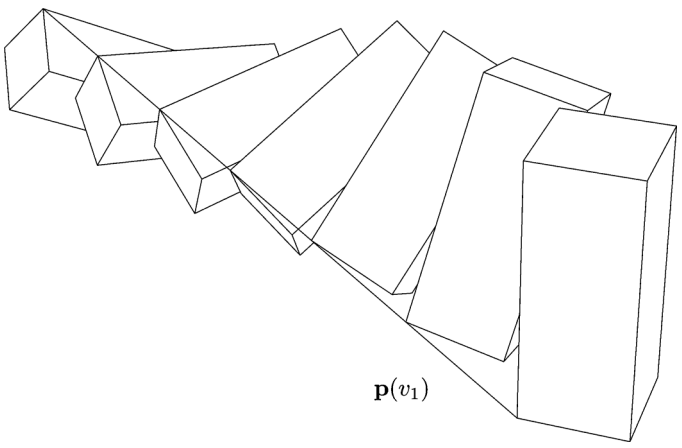

Fig. 7. Symbolic sketch of SM_1.

https://doi.org/10.1017/S0263574707003530 Published online by Cambridge University Press

values of v_1, are drawn as boxes. Through every point of such a 3-space, there is exactly one line that belongs to the manifold.

A lower dimensional example of a Segre manifold is a hyperboloid in E^3, where one has to take two lines instead of the 3-spaces in P^7 and a linear relation between the points on both lines. The lines connecting the corresponding points determine a regulus of a hyperboloid, a Segre manifold in P^3. More generally, a Segre manifold can be defined as a topological product of two linear spaces, i.e., the manifold of all ordered pairs of points of both spaces (see Naas and Schmid).[19]

Definition 1. The Segre manifolds generated by the one parameter set of 3-spaces $T(v_1)$, $T(v_2)$ resp. $T(v_3)$ are denoted by SM_1, SM_2 resp. SM_3. The Segre manifolds generated by the one parameter set of 3-spaces $T_c(v_1)$, $T_c(v_2)$ resp. $T_c(v_3)$ are denoted by SM_{1c}, SM_{2c} resp. SM_{3c}.

Summarizing the findings above one can state:

Theorem 2. *The Segre manifold SM_1 (SM_2, SM_3) is the intersection of four one parameter pencils of hyperplanes. The hyperplane coordinates depend linearly on v_1 (v_2, v_3).*

Furthermore we can state:

Theorem 3. *The constraint manifold of a 3R chain is the intersection of the Study quadric with a Segre manifold SM_1 (SM_2, SM_3) generated by the pencils of hyperplanes describing $T(v_1)$ ($T(v_2)$, $T(v_3)$).*

Corollary 1. *The constraint manifold of a 3R chain is the intersection of any two of the Segre manifolds SM_1, SM_2, SM_3.*

2.2.1. Different representations of the Segre manifold. This section describes different representations of the Segre manifolds SM_i, $i = 1, 2, 3$. As stated above, all three manifolds have the same intersection with S_6^2 and therefore describe the same set of displacements. Note that the difference between the three manifolds are points outside of S_6^2. It has turned out that one has to switch between the different descriptions when special layouts like parallelism of rotation axes occur.

Parametric representation, span of points: Specify one arbitrary 3-space of $T(v_1)$ by fixing the parameter $v_1 = v_{10}$. Choose four linearly independent points $\mathbf{p}_k$ ($k = 1, \ldots, 4$) of this space and then let v_1 vary again (compare Fig. 7). Because of Theorem 1, this results in four straight lines l_k and $\mathbf{p}_k(v_1) = T(v_1) \cap l_k$. Now the points of SM_i are described by

$$\mathbf{x} = \sum_{k=1}^{4} \lambda_k \mathbf{p}_k(v_1)$$

where $(\lambda_1, \lambda_2, \lambda_3, \lambda_4)^T$ is a homogeneous quadruple. In this representation, the algebraic degree of SM_i is easily computed. It is defined as the number of intersection points of SM_i and a generic 3-space $U \subset P^7$ (see Harris[20]). Let U be the span of four points described by $\mathbf{u}_1, \ldots, \mathbf{u}_4$. U and $T(v_1)$ intersect if and only if

$$\det[\mathbf{p}_1(v_1), \mathbf{p}_2(v_1), \mathbf{p}_3(v_1), \mathbf{p}_4(v_1), \mathbf{u}_1, \mathbf{u}_2, \mathbf{u}_3, \mathbf{u}_4] = 0.$$

This is a polynomial of degree four in v_1. Hence, there exist four intersection points of SM_i and U. That means that the algebraic degree of SM_i is four.

Algebraic equations: In order to find a set of algebraic equations of SM_i, one has to fix two parameter values v_{11} and v_{12} and let $\mathbf{p}_{jk} = \mathbf{p}_j(v_k)$ for $j = 1, \ldots, 4$ and $k = 1, 2$. In a projective coordinate frame with base points $\mathbf{p}_{11}, \ldots, \mathbf{p}_{41}, \mathbf{p}_{12}, \ldots, \mathbf{p}_{42}$, one may use the coordinate vectors $(\xi_0 : \cdots : \xi_3 : \eta_0 : \cdots : \eta_3)^T$. In this frame, the algebraic equations of SM_i read

$$\det \begin{bmatrix} \xi_k & \eta_k \\ \xi_l & \eta_l \end{bmatrix} = 0, \qquad k, l, \in \{0, \ldots, 3\} \tag{24}$$

(see Naas *et al.*[19]). Note that only three of these quadric equations are algebraically independent. Therefore, SM_i is contained in the intersection of three hyperquadrics. In order to find the equations of SM_i in the original coordinate frame of P^7, one has to apply the transformation $\mathbf{y} = \mathbf{P}\mathbf{x}$ where $\mathbf{P}$ is the matrix

$$\mathbf{P} = [\mathbf{p}_{11}, \ldots, \mathbf{p}_{41}, \mathbf{p}_{12}, \ldots \mathbf{p}_{42}]$$

to the coordinates in Eq. (24). There exist symmetric 8×8 matrices such that Eq. (24) reads

$$(\xi_0, \ldots, \xi_3, \eta_0, \ldots, \eta_3)^T \cdot \mathbf{A}_{ij} \cdot (\xi_0, \ldots, \xi_3, \eta_0, \ldots \eta_3) = 0.$$

The transformed equations are (see Lemma 4)

$$(\xi_0, \ldots, \xi_3, \eta_0, \ldots, \eta_3)^T \cdot (\mathbf{P}^T)^{-1} \mathbf{A}_{ij} \mathbf{P}^{-1} \cdot (\xi_0, \ldots, \xi_3, \eta_0, \ldots, \eta_3) = 0.$$

Remark 6. It is possible to compute symbolically the system of algebraic equations of all Segre manifolds without specifying the Denavit–Hartenberg parameters.

Intersection of hyperplanes: As investigated in Section 2.1, the constraint manifold of an arbitrary $3R$ chain is the intersection of a one parameter set of 3-spaces, depending linearly on the parameter, with S_6^2. A fixed 3-space in the seven-dimensional projective space is geometrically determined by intersecting four hyperplanes $H_1, \ldots, H_4$. Algebraically, this means it is given by four linear equations. A one parameter set of 3-spaces is therefore given by the intersection of four one parameter sets of hyperplanes $H_i(v)$, $i = 1, \ldots, 4$, each depending linearly on the parameter v. This parameter can be any of the algebraic values of the rotation angles of the $3R$ chain. Such a linear one parameter set of hyperplanes is called a pencil of hyperplanes. For each value of v, the four pencils of hyperplanes intersect in one 3-space of the Segre manifold. The advantage of these hyperplane equations to those presented in Husty *et al.*[13] is that these equations are extremely short (224 operands) because of the newly introduced algorithm although no

https://doi.org/10.1017/S0263574707003530 Published online by Cambridge University Press

Denavit–Hartenberg parameter is specified. Additionally, all the Denavit–Hartenberg parameters appear only multilinear within these equations.

Remark 7. The Segre manifolds have some interesting properties. From the kinematic point of view, the most interesting is the following: The Segre manifolds SM_1, SM_3, and SM_2 (with the restriction that $\alpha_1 = 0$ or $\alpha_2 = 0$; a general SM_2 has different properties that have to be taken into account.[18]) intersect the exceptional generator of S_6^2 (the 3-space, that had to be sliced out of the Segre manifold), given by $x_0 = x_1 = x_2 = x_3 = 0$, in conjugate complex lines. These lines lie in those 3-spaces of the Segre manifolds that correspond to the parameter values $v_i = \pm \mathrm{i}$, $i = 1, 2, 3$. Furthermore, these lines lie on the quadric $y_0^2 + y_1^2 + y_2^2 + y_3^2 = 0$ in this exceptional 3-space.

This property is important because it shows that the exceptional generator plays in spatial kinematics a similar role as the circle points in planar kinematics. A strict proof of the statement above can be found in Pfurner.[18]

2.3. Discussion of the inverse kinematics of general 6R manipulators

In this section, we show how the constraint manifolds of $3R$ chains can be used to solve the inverse kinematics of a general open $6R$ manipulator. Recall that in the inverse kinematics problem of a serial chain, the design and a pose of the end effector of the manipulator are known. The rotation angles u_i of the revolute joints have to be computed.

To apply the theory developed before, one has to break up the link between the third and the fourth revolute axis to obtain two $3R$ chains. It has turned out that the best way to do this is the following: We break up at the foot of the common normal of the third and fourth axes on the fourth axes. Moreover, one has to attach two copies of a coordinate frame $\Sigma_L = \Sigma_R$, called the "left" and the "right" frame, to the resulting mechanisms in the following way:

- The origin is the foot of the common normal of the third and fourth axis on the fourth axis.
- The x-axis is aligned with the common normal of the third and fourth axes.
- The z-axis coincides with the fourth axis.

The resulting mechanisms are two open $3R$ chains, called the "left" and the "right" $3R$ chain. The base frame of the left one is Σ_0 and the end effector frame is Σ_L, the base of the right one is Σ_6 with the end effector Σ_R (see Fig. 8).

The pose of Σ_L with respect to Σ_0 is given by

$$\mathbf{T}_1 = \mathbf{M}_1 \cdot \mathbf{G}_1 \cdot \mathbf{M}_2 \cdot \mathbf{G}_2 \cdot \mathbf{M}_3 \cdot \mathbf{G}_3. \tag{25}$$

This is exactly the canonical $3R$ chain for which the canonical constraint manifold was developed. This manifold was the intersection of one of the Segre manifolds SM_{1c}, SM_{2c}, or SM_{3c} resp. the intersection of one of the 3-spaces T_{cp} or T_{cw} with the Study quadric. Which one of the constraint manifolds has to be taken depends on the Denavit–Hartenberg parameters of the $6R$ manipulator, because in

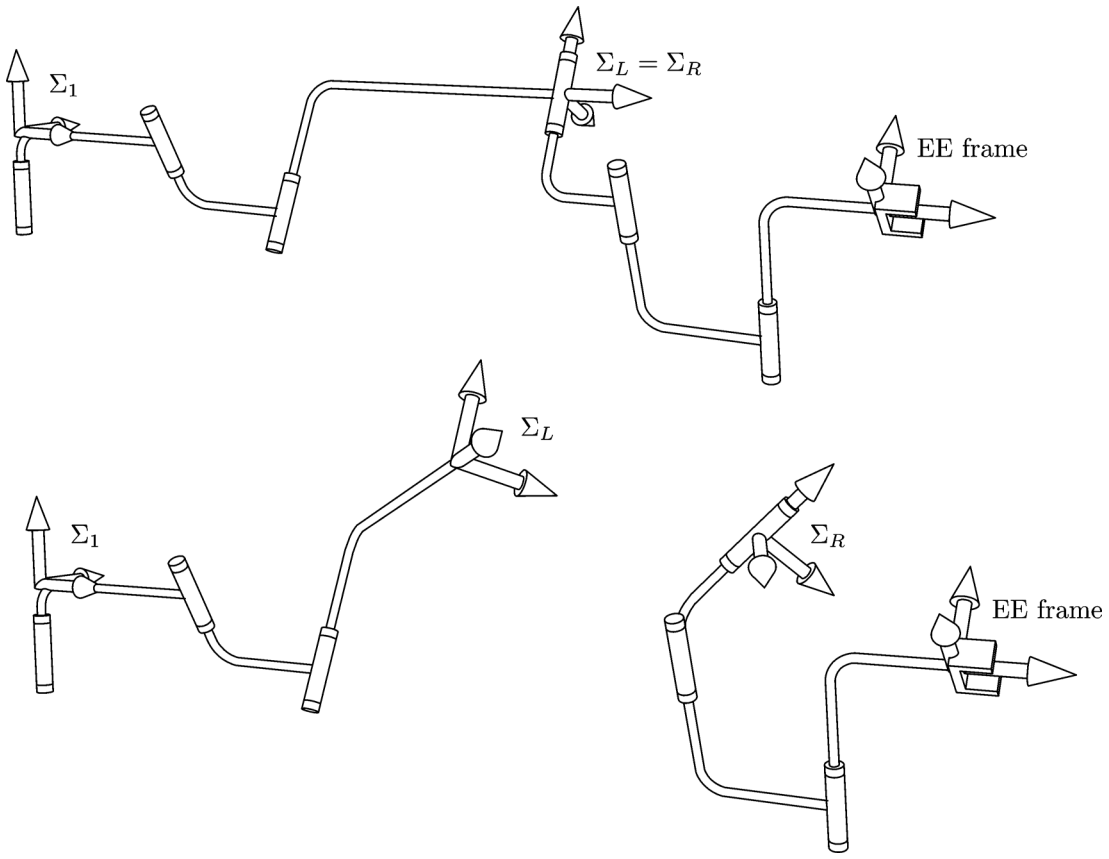

Fig. 8. Cutting of the $6R$ into two $3R$ serial chains.

https://doi.org/10.1017/S0263574707003530 Published online by Cambridge University Press

some special cases one or more of the Segre manifolds lie completely on S_6^2.

The pose of Σ_R with respect to Σ_6 is given by

$$\mathbf{T}_2 = \mathbf{A} \cdot \mathbf{G}_6^{-1} \cdot \mathbf{M}_6^{-1} \cdot \mathbf{G}_5^{-1} \cdot \mathbf{M}_5^{-1} \cdot \mathbf{G}_4^{-1} \cdot \mathbf{M}_4^{-1}. \quad (26)$$

To achieve the representation of the constraint manifold of this right $3R$ chain, one has to take the hyperplane equations representing $T(v_1)$, $T(v_2)$, and $T(v_3)$ for an arbitrary design or the hyperplane equations representing T_p in Eqs. (23) resp. T_w for special designs.

Pfurner[18] has shown that one can adapt the coordinate systems slightly to get the simplest set of equations. After these substitutions, the one parameter sets of 3-spaces are denoted by $T(v_6)$, $T(v_5)$ resp. $T(v_4)$, and each of them describes also a Segre manifold denoted by SM_6, SM_5 resp. SM_4. Each of them can serve as SM_R. The four pencils of hyperplanes corresponding to each Segre manifold are denoted by $H_5(v_i), \ldots, H_8(v_i)$ for $i = 4, 5, 6$. The representations of the fixed 3-spaces are denoted by $\overline{T}_p$ and $\overline{T}_w$.

The solution of the inverse kinematics problem of a serial $6R$ chain can therefore be computed as the intersection

$$S_6^2 \cap SM_L \cap SM_R. \quad (27)$$

One can summarize these results in:

Theorem 4. *Geometrically, the solution of the inverse kinematic problem of a serial 6R chain is equivalent to the intersection of eight one parameter sets of hyperplanes with S_6^2 in P^7.*

An investigation of the structure of the nine equations addressed in Theorem 3 reveals the nonlinearity of the problem. There are eight hyperplane equations H_i, which are linear in x_i, y_i and bilinear in $x_i v_q$ and $y_i v_q$, respectively $x_i \overline{v}_r$ and $y_i \overline{v}_r$, $i = 0, \ldots, 3$. v_q denotes the tangent half of one of the revolute joints of the left $3R$ chain and may therefore be one of the numbers 1, 2, 3 depending on the structure of the $3R$ chain. $\overline{v}_r$ denotes the tangent half of one of the revolute joints of the right $3R$ chain and may therefore be one of the numbers 4, 5, 6 depending on the structure of the $3R$ chain. Eq. (4) of S_6^2 is bilinear in x_i and y_i, $i = 0, \ldots, 3$.

The solution algorithm of this intersection problem is straight forward. At first, one normalizes the Study parameters by setting one suitable coordinate, say x_0, equal to one (at least one has to be nonzero!). The remaining seven Study parameters are solved linearly from seven arbitrary hyperplane equations, say $H_1, \ldots, H_7$.

Remark 8. It should be mentioned here that it is possible to solve the set of linear equations in full generality, that means without setting the Denavit–Hartenberg parameters. But the output of the solution is that big that it does not make sense to operate with this solution. It is much faster to substitute the Denavit–Hartenberg parameters before solving the linear system.

Multiplying the solutions for the Study parameters by the common denominator yields all Study parameters depending on the two parameters v_q and $\overline{v}_r$

$$x_i = x_i(v_q, \overline{v}_r), \quad y_i = y_i(v_q, \overline{v}_r). \quad (28)$$

Substituting these Study parameters into Eq. (4) and into the one remaining equation H_8 one obtains two nonlinear algebraic equations $E_1 = 0$ and $E_2 = 0$ in the two parameters

$$E_1(v_q, \overline{v}_r) = 0, \quad E_2(v_q, \overline{v}_r) = 0.$$

Remark 9. The vanishing of E_2 is the condition for intersecting the two one parameter sets of 3-spaces $T_c(v_q)$ and $T(\overline{v}_r)$ of SM_L and SM_R described by $H_1, \ldots, H_4$ and $H_5, \ldots, H_8$. Hence, it can be also written as the determinant

$$\det[\mathbf{h}_1, \mathbf{h}_2, \mathbf{h}_3, \mathbf{h}_4, \mathbf{h}_5, \mathbf{h}_6, \mathbf{h}_7, \mathbf{h}_8] = 0 \quad (29)$$

where $\mathbf{h}_i$ are the hyperplane coordinates of H_i for $i = 1, \ldots, 8$.

The resultant of E_1 and E_2 with respect to one unknown, e.g. $\overline{v}_r$, yields a univariate polynomial of degree 56 in the remaining unknown v_q. This polynomial factors into

$$\left(1 + v_q^2\right)^4 \mathcal{P}_1(v_q) \mathcal{P}_2(v_q) \mathcal{P}_3(v_q)^2 \mathcal{P}(v_q) = 0.$$

$(1 + v_q^2)$ yields the solutions $v_q = \pm \mathrm{i}$, which belong to points in the exceptional generator and can be therefore canceled. The polynomials $\mathcal{P}_1$ and $\mathcal{P}_2$ are of degree four in v_q and belong, after back substitution of the roots and comparing the common roots of E_1 and E_2, to solutions $\overline{v}_r = \pm \mathrm{i}$. Therefore, these two polynomials can also be canceled. $\mathcal{P}_3$ is a polynomial of degree 12 and belongs to values of v_q that yield, back substituted into the solved linear system, solutions of the form $(0 : 0 : 0 : 0 : 0 : 0 : 0 : 0)$. This point is excluded from P^7 and therefore $\mathcal{P}_3$ can also be omitted from this polynomial. $\mathcal{P}$ is the univariate polynomial of degree 16.

Remark 10. The resultant factors are in the described way in the general case. In special cases, the factorization may look different, but the factors which do not solve the whole system can always be excluded with the same statements.

Remark 11. For every design, it is possible to compute the univariate polynomial in a short time exactly. It depends on the degree of the polynomial if the roots can be obtained in closed form or only numerically.

Solving $\mathcal{P}$ for the unknown v_q yields 16 roots over $\mathbb{C}$. The other unknowns can be computed by back substitution of these solutions into E_1 and E_2. Solving both equations and comparing the solutions yields one common solution of the system for $\overline{v}_r$. Note that the solution of these equations are already the algebraic values of two of the joint angles of the $6R$ mechanism. Having the values of these two unknowns, one can substitute the 16 pairs of solutions into the Study parameters that resulted from the solutions of the linear system in Eq. (28). This yields 16 poses where the right and the left coordinate systems coincide ($\Sigma_L = \Sigma_R$).

The remaining task is simple: One has to compute the inverse kinematics of two $2R$ chains. To do this, one has to

https://doi.org/10.1017/S0263574707003530 Published online by Cambridge University Press

compare the entries of the matrices describing the motion of the remaining $2R$ chains $\mathbf{T}_1(u_1, u_2, u_3)$ (where one of the joint variables is fixed) in Eq. (25) and $\mathbf{T}_2(u_4, u_5, u_6)$ (where one of the joint variables is fixed) in Eq. (26), with the entries of the matrix that describe the pose of $\Sigma_L = \Sigma_R$. This leads to an overdetermined set of equations for the four unknown angles.

Theorem 1 gives another possibility to solve the inverse kinematics of the remaining $2R$ chains. For every $3R$ chain one has, in general, three different Segre manifolds to obtain the constraint manifold. For the derivation of the poses where $\Sigma_L = \Sigma_R$, we have used only one of them. The computed solutions have to be on all Segre manifolds. Using this fact one can obtain linear equations in the remaining four unknowns from the remaining four Segre manifolds.

Overconstrained 6R-Mechanisms: In case that E_1 or E_2 vanish or the resultant of E_1 and E_2 vanishes, we cannot create a univariate polynomial in one of the remaining unknowns. The $6R$ chain is overconstrained. The remaining equation or the common factor determines the one parameter motion of the chain (see Pfurner and Husty[21]).

3. Synthesis of Mechanisms

Kinematic mapping can also be used in the synthesis of mechanisms. A detailed introduction into this interesting topic can be found in McCarthy.[6] The mathematical tools used there are closely related to the methods presented within this paper. But there is a difference in the geometric interpretation of the derived equations. We show the application of our methods in the synthesis of a Bennett mechanism.

The Bennett mechanism is a closed $4R$ chain. It is well known that a Bennett mechanism can be synthesized exactly when three poses of the end effector system are given (Fig. 9). Synthesis means that we have to find the design parameters of the mechanism and the location of the axes in the fixed system and the location of the moving body in the moving system. For the synthesis of such a mechanism, we attach two of the revolute axes to the fixed system and two axes to the moving (coupler) system. Now we prize open the coupler link and obtain two open $2R$ chains. The basic idea of the synthesis is to map the possible displacements of the first $2R$ chain onto S_6^2. This yields the constraint manifold M_1 of the $2R$ chain in the kinematic image space. We perform the same procedure with the other $2R$ chain and obtain a second constraint manifold M_2. Possible assembly modes of the two $2R$ chains correspond to intersection points of M_1 and M_2.

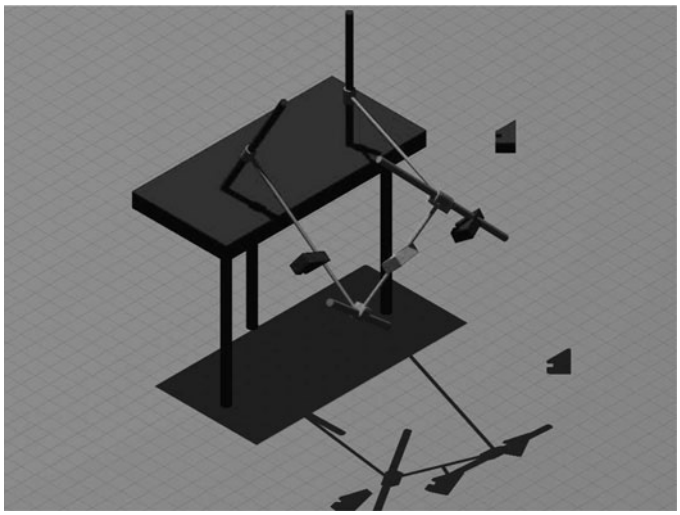

Fig. 9. Bennett mechanism.

Due to the fact that a Bennett mechanism consists of two $2R$ chains, one has to intersect two 3-spaces L_1^3, L_2^3 in P^7. According to the well-known dimension formula

$$\dim(U \cap V) = \dim(U) + \dim(V) - \dim(U + V) \quad (30)$$

where U, V denote subspaces of an n-dimensional space P^n, the intersection of two 3-spaces L_1^3, L_2^3 in a seven-dimensional space P^7 can be

- $\dim(L_1^3 \cap L_2^3) = -1, \Rightarrow$ intersection is empty,
- $\dim(L_1^3 \cap L_2^3) = 0, \Rightarrow$ intersection is one point,
- $\dim(L_1^3 \cap L_2^3) = 1, \Rightarrow$ intersection is a line,
- $\dim(L_1^3 \cap L_2^3) = 2, \Rightarrow$ intersection is a two-plane,
- $\dim(L_1^3 \cap L_2^3) = 3 \Rightarrow L_1^3$ and L_2^3 coincide.

The first case is the general case. The mechanical interpretation is that two general $2R$ chains never can be assembled to form a closed $4R$ mechanism. There have to be conditions to make this happen. When the constraint manifolds are chosen such that they come from a $4R$ chain, then they have exactly one point in common, which is on S_6^2 (forward kinematics of a serial $4R$ chain). This fact is also a simple proof that the inverse kinematics of a general $4R$ serial chain has one solution. The case of the line intersection is only possible for special $4R$ chains for which the inverse kinematics then has two solutions, which correspond to the two intersections of the line with S_6^2. As we know, the Bennett motion is a one-parameter motion, represented by a curve in the kinematic image space. Therefore, only the cases of a line, which lies completely on S_6^2 or a two-plane are of interest. The case that the line is contained in S_6^2 is not possible. Following Baker,[22] who argued via screws, the relative motion between opposite links of a proper Bennett loop can be neither purely rotational nor purely translational at any time. Since straight lines on S_6^2 correspond to rotations or translations, we can restrict ourselves to the case of $\dim(L_1^3 \cap L_2^3) = 2$. The kinematic image of the Bennett motion is therefore the intersection of a two-plane with the Study quadric S_6^2. This yields another confirmation of the fact that the synthesis of a Bennett needs three precision points. Three precision points correspond to three points on the Study quadric and span the two-plane. This agrees with Suh and Radcliffe.[23] To summariz we have:

Theorem 5. *Bennett motions are represented by planar sections of the Study quadric and vice versa.*

The intersection of the two-plane and S_6^2 is a quadratic curve. In this sense, Bennett motions can be regarded as the simplest nontrivial one parameter space motions. A direct consequence of the above considerations is the following:

Corollary 2. *Bennett linkages are the only movable* $4R$ *chains* (*apart from planar and spherical* $4R$ *chains*).

https://doi.org/10.1017/S0263574707003530 Published online by Cambridge University Press

It should be noted that to the authors' best knowledge, up to now there exist only complicated algebraic proofs of this result (A. Karger, private communication).

Synthesis algorithm: Given are three precision points A, B, $C \in S_6^2$, corresponding to three poses of a coordinate system. The goal is to compute the design parameters of the Bennett mechanism that guides the coupler system through these poses. The above mentioned theorem states that the Bennett motion corresponds to the conic on S_6^2 passing through A, B, and C. This conic can be parameterized rationally according to

$$\mathbf{f}(s) = \mathbf{p}_0 + s\mathbf{p}_1 + s^2\mathbf{p}_2, \qquad \mathbf{p}_0, \mathbf{p}_1, \mathbf{p}_2 \in \mathbb{R}^8.$$

Applying inverse kinematic mapping by substituting the components of the vector function $\mathbf{f}(s)$ into Eq. (2) yields a rational parameterization $\mathbf{M}(s)$ of the Bennett motion. The trajectory of a point having homogeneous coordinates $(1, x_1, x_2, x_3)^T$ is the rational quartic

$$\mathbf{c}(s) := (X_0, X_1, X_2, X_3)^T(s) = \mathbf{M}(s)(1, x_1, x_2, x_3)^T. \quad (31)$$

After this step of the algorithm, the motion of the coupler system of the synthesized Bennett mechanism is determined. For the mechanical design, the axes and the Denavit–Hartenberg parameters of the mechanism are necessary. To compute the parametric representation of the axes, we follow the procedure developed in Bottema and Roth,[10] in a slightly modified and adapted way. This is necessary because the motion is not given in the canonical form on which the geometric arguments in Bottema and Roth,[10] are based. In Bottema and Roth[10] it is shown that there exist two pairs of conjugate complex isotropic planes ψ_i, $\overline{\psi_i}$ $(i = 1, 2)$ whose points have trajectories of degree three or lower. Their pairwise intersections consist of four complex and two real lines. The two real lines are the moving axes of the Bennett mechanism and the paths of points on these lines are circles. The circles are in parallel planes having centers on common axes, the two real circle axes are the fixed axes of the mechanism. From Eq. (31) it is known that all trajectories $\mathbf{c}(s)$ are parameterized with rational functions of degree four. This is also true for the cubic trajectories and the circles. The only possibility to obtain a rational parameterization of degree four for twisted cubics is degree elevation of a rational cubic parameterization. Therefore, in case of a cubic trajectory, the parametric representation can be written in the form

$$\mathbf{c}(s) = (s - \widetilde{s})\widetilde{\mathbf{c}}(s) \quad (32)$$

where $\widetilde{s} \in \mathbb{R}$ is constant and $\widetilde{\mathbf{c}}(s)$ consists of cubic polynomials. We have to determine points in the moving system such that they have common zeros of all of their coordinate functions. As we know from above, the solutions will be the points in the planes ψ_i and $\overline{\psi_i}$. Since the homogenizing coordinate $X_0(s)$ is independent of x_1, x_2, and x_3, we can compute the zeros of this function. It turns out that the four zeros are pairwise conjugate complex s_1, $\overline{s_1}$, s_2 and $\overline{s_2}$. The equations of the isotropic planes are found by substituting s_i and $\overline{s_i}$ in either $X_1(s)$, $X_2(s)$, or $X_3(s)$. The computation of the mechanism's fixed and moving axes is now elementary. The implementation of this algorithm is straightforward. The most expensive step is solving the quartic equation $X_0(s) = 0$. As opposed to previous solutions, for example Perez,[24] no system of equations has to be solved and no discussion of reality of roots is necessary.

A second possibility to determine the axes is to compute the points which have planar trajectories because these points are on the moving axes. If the trajectory of a certain point is planar, the torsion of the trajectory has to vanish for all parameter values t. Following Husty *et al.*,[5] the torsion is given by

$$\tau = \frac{\left|\frac{d\mathbf{c}(t)}{dt}, \frac{d^2\mathbf{c}(t)}{dt^2}, \frac{d^3\mathbf{c}(t)}{dt^3}\right|}{\left|\frac{d\mathbf{c}(t)}{dt} \times \frac{d^2\mathbf{c}(t)}{dt^2}\right|^2}.$$

$\tau = 0$ means that

$$\frac{d\mathbf{c}(t)}{dt}, \frac{d^2\mathbf{c}(t)}{dt^2}, \frac{d^3\mathbf{c}(t)}{dt^3}$$

have to be linearly dependent. Therefore, the numerator of the determinant, which is a function in t of degree 4, has to vanish identically for points on the moving axes. That means that all five coefficients of this polynomial have to vanish. Each coefficient is a cubic polynomial in the coordinates (x_1, x_2, x_3) of the moving point. This gives a system of five equations $F = \{G_0, \ldots, G_4\}$, which is solvable but has an infinite number of solutions, exactly as we expect.

For F a Gröbner basis can be determined. It turns out that the Gröbner basis contains only four polynomials $A = \{B_0, \ldots, B_3\}$. The moving axes belong to the zero-set of A, which is determined with the help of resultants. Every possible resultant yields a polynomial of degree nine, which factors in a polynomial of degree three and one of degree six. The geometric interpretation of this fact is the following: The zeros of each of the cubic polynomials determine a cubic surface in the moving space. These cubic surfaces have six lines in common and three pairwise different points. Two of the six lines are real. The axes in the fixed space can be computed via the centers of the paths of the moving axes. For a numerical example, we have to refer to Brunnthaler.[25,26]

4. Conclusion

In this overview, we have discussed the application of kinematic mapping and the resulting geometric-algebraic approach to solve problems in mechanism analysis and synthesis. It was shown that geometric preprocessing in a multidimensional setting allowed to simplify and subsequently solve the sets of polynomial equations linked to the mechanical problems.

References

1. J. Angeles, *Fundamentals of Robotic Mechanical Systems. Theory, Methods and Algorithms* (Springer, New York, 1997).
2. A. Dickenstein and I. Z. Emiris, *Solving Polynomial Equations, Foundations, Algorithms and Applications* (Springer, New York, 2005).

https://doi.org/10.1017/S0263574707003530 Published online by Cambridge University Press

3. W. Blaschke, *Kinematik und Quaternionen*. Mathematische Monographien (Springer, Berlin, 1960).
4. E. Study, *Geometrie der Dynamen* (B. G. Teubner, Leipzig, 1903).
5. M. L. Husty, A. Karger, H. Sachs and W. Steinhilper, *Kinematik und Robotik* (Springer, Berlin, Heidelberg, New York, 1997).
6. J. M. McCarthy, *Geometric Design of Linkages*, *Interdisciplinary Applied Mathematics* (Springer, New York, 2000) vol. 320.
7. J. M. Selig, *Geometric Fundamentals of Robotics. Monographs in Computer Science* (Springer, New York, 2005).
8. O. Giering, *Vorlesungen über höhere Geometrie* (Vieweg Verlag, Braunschweig, 1983).
9. M. Husty, "On the Workspace of Planar Three-Legged Platforms," *Proceedings of the ISRAM – World Congress of Automation*, Montpellier, France (1996) pp. 1790–1796.
10. O. Bottema and B. Roth, *Theoretical Kinematics* (Dover, New York, 1990).
11. K. Brunnthaler, M. Pfurner and M. Husty, "Synthesis of planar four-bar mechanisms," *CSME Trans.* **30**(2), 297–313 (2006).
12. M. Husty, M. Pfurner and H.-P. Schröcker, "A New and Efficient Algorithm for the Inverse Kinematics of a General Serial 6R," *Proceedings of ASME 2005 29th Mechanism and Robotics Conference,* Long Beach (2005).
13. M. Husty, M. Pfurner and H.-P. Schröcker: "A new and efficient algorithm for the inverse kinematics of a general serial 6R manipulator," *Mech. Mach. Theory* **42**(1), 66–81 (2007).
14. M. Husty: "An algorithm for solving the direct kinematic of general Stewart–Gough platforms," *Mech. Mach. Theory* **31**(4), 365–380 (1996).
15. M. Husty and A. Karger, "Self-Motions of Griffis-Duffy Type Platforms," *Proceedings of IEEE Conference on Robotics and Automation*, San Francisco (2000) pp. 7–12.
16. M. Husty and A. Karger, "Self Motions of Stewart–Gough Platforms, an Overview," *Proceedings of the Workshop on Fundamental Issues and Future Research Directions for Parallel Mechanisms and Manipulators*, Quebec City (2002) pp. 131–141.
17. J. Denavit and R. S. Hartenberg, "A kinematic notation for lower-pair mechanisms based on matrices," *J. Appl. Mech.* **77**, 215–221 (1955).
18. M. Pfurner, Analysis of Spatial Serial Manipulators Using Kinematic Mapping. *Ph.D. Thesis* (Innsbruck: Universität Innsbruck, 2006).
19. J. Naas and H. L. Schmid, *Mathematisches Wörterbuch, Band II* (Akademie-Verlag Berlin, 1974).
20. J. Harris, "Algebraic Geometry: A First Course," *In: Graduate Texts in Mathematics* (Springer, New York, 1995) vol. 133.
21. M. Pfurner and M. Husty, "Determining the Motion of Overconstrained 6R Mechanisms," *Proceedings of the IFToMM World Congress*, Besançon (2007) to be published.
22. J. E. Baker, "On the Motion Geometry of the Bennett Linkage," *Proceedings of the 8th International Conference on Engineering Computer Graphics and Descriptive Geometry*, Austin, Texas (1998) pp. 433–437.
23. C. H. Suh and C. W. Radcliffe, *Kinematics and Mechanisms Designs* (Wiley, Canada, 1978).
24. A. Perez, Analysis and Design of Bennett Linkages. *Ph.D. Thesis* (Irvine, CA: University of California, 2004).
25. K. Brunnthaler, Synthesis of 4R Linkages Using Kinematic Mapping. *Ph.D. Thesis* (Innsbruck: Universität Innsbruck, 2007).
26. K. Brunnthaler, H.-P. Schröcker and M. L. Husty, "A New Method for the Synthesis of Bennett Mechanisms," *Proceedings of CK 2005*, Cassino, Italy (2005).

https://doi.org/10.1017/S0263574707003530 Published online by Cambridge University Press